



$\text{Al}_2\text{O}_3/\text{Fe}_3\text{O}_4/\text{ZrO}_2$ Ternary Nanosorbent: Synthesis and Characterization for Organic Dyes and Toxic Heavy Metals Removal from Wastewater

D.L. Wubishet^a, T.M. Abi^b, D.T. Fekadu^b

^aSchool of Natural Resource Management and Environmental Sciences, Haramaya University, Haramaya, Ethiopia.

^bDepartment of Chemistry, Haramaya University, Haramaya, Ethiopia.

Received 26 May 2020,
Revised 21 July 2020,
Accepted 23 July 2020

Keywords

- ✓ Adsorption,
- ✓ Organic dyes,
- ✓ Heavy metals,
- ✓ Ternary oxide nanosorbent

bokhallel@yahoo.fr
Phone: +213797906845

Abstract

Dyes and heavy metals are among contaminants released to our water bodies through various activities. Some of these dyes and heavy metals are toxic, carcinogenic, and can cause potential hazards to environment. Therefore finding the robust techniques to remove them from our water is mandatory. In the present study the $\text{Al}_2\text{O}_3/\text{Fe}_3\text{O}_4/\text{ZrO}_2$ ternary nanosorbent was prepared by co precipitation method to remove dyes (methyl orange and methylene blue) and heavy metals (Cu, Ni and Zn) from wastewater. This nanosorbent was characterized by using modern instruments such as, BET, XRD, FTIR and SEM-EDX. The study investigated the effect of different parameters such as, effect of solution pH, amount of adsorbent dose, contact time, initial concentration of MB, MO, Cu, Zn and Ni. Desorption of MO, MB, Cu, Zn and Ni from the nanosized adsorbent and recyclability of the sorbent was also investigated. The adsorption of MO, Cu, Zn and Ni was maximum at pH 6 and that of MB was at pH 4. This confirms that dependency of adsorption process on pH. Both Langmuir and Freundlich models were able to sufficiently describe the sorption data of the elements as indicated by R^2 values of > 0.9 . The adsorption of all elements is spontaneous and follows pseudo second order reaction as indicated by thermodynamic and adsorption kinetic study respectively.

1. Introduction

Water is one of the vital necessities for the survival of human beings. Earth is a planet with 71% of its surface covered by water. Of the total available water on earth 97% is seawater and unavailable for human consumption, only 3% is available as fresh water. Many countries are facing the shortage of clean drinking water and it is estimated that 1.2 billion people are already drinking unclean water. Furthermore, 5-10 million people die annually due to various diseases caused by the consumption of contaminated water. The increasing demand of clean water has attracted much of the attention of government organizations and water industries to develop cost-effective technologies for water/wastewater treatment and reclamation [1].

The rapid industrialization and urbanization result in the discharge of large amounts of waste to the environment, which in turn creates more pollution. Majority of colored effluents consist of dyes, released to the environment from textile, dyestuff and dyeing industries. Dye is carcinogenic, affects reproductive organs and develops toxicity and neurotoxicity. Therefore, there is an urgent requirement for development of innovative, but low-cost processes by which dye molecules can be removed [2]. Heavy metals are also another contaminants introduced to our water sources. The most common toxic heavy metals in wastewater include arsenic, lead, mercury, cadmium, chromium, copper, nickel, silver, and zinc. The release of high amounts of heavy metals into water bodies creates serious health and environmental problems and may lead to an upsurge in wastewater treatment cost. Their occurrence and accumulation in the environment is a result of direct or indirect human activities, such as rapid industrialization, urbanization and anthropogenic sources [3].

Different methods have been used for removal of contaminants from wastewater. They mainly include: precipitation, ion exchange, membrane processes, evaporation, chemical oxidation or reduction, solvent extraction and biological materials. These techniques are very expensive and economically unfavorable or technically complicated, and are used only in special cases of wastewater treatment. Relatively a new green technology for the treatment of industrial wastewater is adsorption of heavy metals and dyes from aqueous solutions by using adsorbents. Adsorption process has been proved to be an excellent way to treat industrial waste effluents, offering significant advantages like low cost, availability, profitability, easy operation and efficiency [4]. Nanomaterials typically exhibit unique electronic, optical and mechanical properties compared to their bulk counterpart and even molecular complements. They have large surface area than bulk materials, enhanced reactivity self assembly and their wider availability make them particularly attractive separation media for water purification [5].

In the present study magnetic $\text{Fe}_3\text{O}_4/\text{Al}_2\text{O}_3/\text{ZrO}_2$ ternary nanoparticle was prepared by chemical coprecipitation method for the removal of organic dyes (methyl blue, Methyl orange) and Heavy metals (Copper, Zinc, Ni) wastewater. Magnetic materials have gained special attention in water treatment, based on their advantage such as easy separation, simple manipulation process, kind operation conditions and easy specifically functional modifications [6]. Magnetite (Fe_3O_4)-based nanomaterials could be easily separated from the aqueous solution after treatment by adding a magnetic field [7]. Zirconium oxides based nanosized materials are another kind of promising metallic oxides adsorbent which can be used to remove contaminants from wastewater. Their advantages are that they have plenty of OH on their surfaces and possess large surface areas. Moreover, nanosized zirconium oxides own great chemical stabilities and exhibit excellent adsorption affinities towards heavy metals. These motivated us to work on adsorption of these dyes and heavy metals from aqueous solution [8].

Therefore, the main objective of the present study was to study the sorption behavior of $\text{Al}_2\text{O}_3/\text{Fe}_3\text{O}_4/\text{ZrO}_2$ sorbent for removal of two organic dyes (MO, MB) and three heavy metals (Cu, Zn, Ni) from waste water. The adsorption behavior of this nanoparticle towards MB, MO, Cu, Zn and Ni was investigated under different conditions, such as pH, contact time, dose, initial adsorbate concentration, agitation speed and temperature.

2. Methodology

2.1. Preparation of Standard Solution

1000 mg/L of stock solutions of methylene blue, methyl orange, copper, zink and nickel were prepared by dissolving $\text{C}_{16}\text{H}_{18}\text{ClN}_3\text{S}\cdot 3\text{H}_2\text{O}$, $\text{C}_{14}\text{H}_{14}\text{N}_3\text{NaO}_3\text{S}$, $\text{CuSO}_4\cdot 5\text{H}_2\text{O}$, ZnCl_2 and $\text{NiCl}_2\cdot 6\text{H}_2\text{O}$ respectively

in 1000 ml distilled water. All experimental solutions were prepared by diluting the stock solution to the required concentration. The pH of each experimental solution was adjusted to the required initial pH value using dilute HCl (or) NaOH [9].

2.2. Synthesis Procedure of the Adsorbents

Al₂O₃/Fe₃O₄/ZrO₂ ternary oxide nanocomposite was prepared by chemical co-precipitation in Fe:Al:Zr mole ratio of 70:25:5 respectively. In the first phase Fe₃O₄ magnetic nanoparticles was prepared by co-precipitation of ferric and ferrous salts under the presence of N₂ gas. 15.1 g FeCl₃ and 5.55 g of FeCl₂ were dissolved in 100 mL of 0.3M HCl [10]. Then, the solution was added drop wise from separatory funnel into the solution of 120 mL of 3M NaOH over a period of 2 h, under vigorous stirring at 80°C in N₂ atmosphere [10]. The magnetite–alumina–zirconia oxide nanocomposite was prepared by adding stoichiometrically calculated amount of Al(NO₃)₃.9H₂O and ZrOCl₂ into the obtained Fe₃O₄. Then, the mixture was stirred under N₂ atmosphere for 1.5 h at 70°C by adjusting pH of the mixture to 8. After several washing the mixture was dried at 60-70°C for 24 h to obtain the desired product [11].

2.3. Characterization of the As-synthesized Powder

The crystalline phases were determined using X-ray diffraction (XRD) technique. The surface functional groups of the nanocomposite, surface area and morphology were determined by FTIR, BET and SEM-EDX respectively.

2.4. Batch Adsorption procedure

The batch experiments to evaluate the ability of Al₂O₃/Fe₃O₄/ZrO₂ to remove these heavy metals and dyes from aqueous solution were carried out in 250 mL conical flask containing 50 mL of 30 mg/L of each adsorbate solution [12]. The MB and MO concentration were determined at wavelength of 661 nm and 464 nm using UV VIS spectrophotometer respectively. Cu, Ni and Zn were determined by flame atomic absorption spectroscopy.

The dye/heavy metal removal efficiency (R) and the amount of dye/heavy metal adsorbed per unit mass of adsorbent at time t (q_t, mg g⁻¹) and at equilibrium (q_e, mg g⁻¹) were calculated using the following equation:

$$\% \text{ Adsorption (R)} = \frac{(C_0 - C_e)}{C_0} \times 100 \quad (1)$$

$$\text{Adsorption Capacity (q}_e) = \frac{(C_0 - C_e)}{w} \times V \quad (2)$$

$$\text{Adsorption Capacity (q}_t) = \frac{(C_0 - C_t)}{w} \times V \quad (3)$$

Where C_t (mg/L) is the concentration of dye/Metal ion at time t and C₀ and C_e (m/L) are the initial and equilibrium concentrations of the dye/metal ion solution respectively. q_e(mg/g) represents the amount of dye/metal adsorbed onto the adsorbent at equilibrium, V(mL) is the volume of the dye/metal solution and W (g) is the amount of the adsorbent [13].

2.4.1. Determination of the pH of Point Zero Charge (pHPZC)

50 mL of 0.001M NaNO₃ solution was added into six different 250 mL polyethylene flasks and the pH of each content was adjusted to various pH values ranging from 2-12. Then the pH of point zero charge

was determined according to [14], by plotting the graph of pH (final-initial) (Y-axis) vs pH final (X-axis).

2.4.2. Effect of Solution pH, Adsorbent Dosage, Contact time, Agitation Speed and initial concentration study.

The effect of pH solution on removal of MO, MB, Cu, Ni and Zn was investigated in the pH range from 2 to 10 (Yan and Wang, 2013). 50 mL of initial concentration of 30 mg/L of the adsorbate was mixed with 0.1g of the adsorbent dose and agitated at 120 rpm for 8 h. Effect of adsorbent dosage (0.05-2 g), [15], contact time (4-24 hour), agitation speed (50-200 rpm) and initial concentration (10-100 mg/L) using pre optimized pH value were investigated.

2.4.3. Adsorption Isotherm, Adsorption kinetics and Thermodynamic Study

Data for plotting isotherm was obtained by mixing concentration ranging from 10-100 mg/L. Adsorption kinetics and thermodynamic feasibility of the sorption process was investigated by varying time from 4-24 and temperature from 20-60 °C respectively at predetermined and optimized values of parameters.

2.4.4. Desorption and Applicability on Real Water Samples Treatment Study

To investigate desorption of the adsorbate from the exhausted adsorbent, the optimized adsorbent dose was subjected to adsorption for optimized hour. Then the exhausted adsorbent was conditioned (immersed) in 50 mL of 0.1 M NaOH, 0.1M HCL and Deionized water solutions for desorption to take place [16]. MO, MB, Cu, Ni and Zn removal capability of the nanosorbent from actual water samples was evaluated on waste water collected from Harar beer factory, Harar city, Ethiopia. First the initial concentration of this adsorbate in these water samples was determined before loading the adsorbent. Then the synthesized nano sorbent was mixed with 50 mL of these water samples at optimized condition to see its removal capacity. For Organic dyes contaminated aqueous solutions were artificially prepared by adding 5 ppm into the water.

3. Results and Discussions

3.1. Characterization of the Adsorbent

3.1.1. Surface Area

The specific surface area of the as-synthesized adsorbent was determined from both single point and multipoint Brunauer–Emmett–Teller (BET) N₂ adsorption and desorption isotherms. This study provided the specific surface area of Al₂O₃/Fe₃O₄/ZrO₂ ternary oxide which was found to be 205.1602 m²/g. The high specific surface area may have resulted from the presence of zirconium (ZrO₂) oxides as reported by [17]. Nanomaterials with high surface activity, high specific surface area and high surface energy show promising potential for the preparation of a high-performance adsorbents having wide application [18].

3.1.2. Powder X-ray diffraction

The XRD patterns of the Al-Fe-Zr ternary oxide nanocomposite before adsorption experiments were demonstrated and presented on Figure 1.

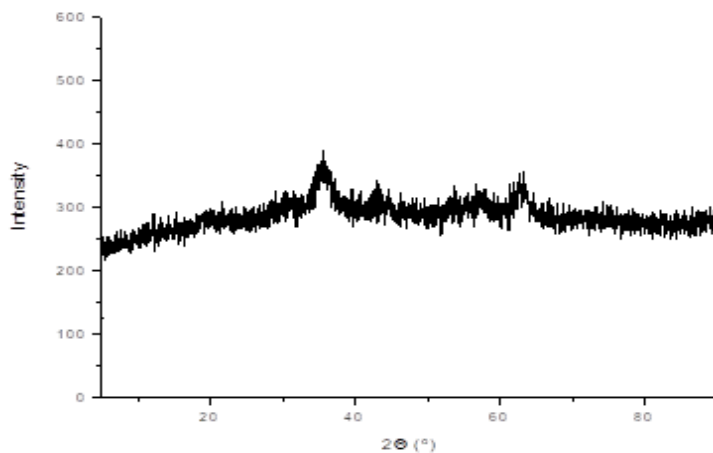


Figure 1. XRD pattern of the as-synthesized $\text{Al}_2\text{O}_3/\text{Fe}_3\text{O}_4/\text{ZrO}_2$ mixed oxide

The diffraction pattern shows weak intensities on a broad background suggesting the amorphous nature of the adsorbent. However, the presence of some low intensity peaks at 2θ values of 35.25 , 43.42 and 63.33° were observed. This indicates that the formation of some crystallites at very small scale up on composite formation. The indicated peaks could be assigned to a face centered cubic spinel structure of pure magnetite (Fe_3O_4). This result agrees with pure standard Fe_3O_4 [19]. No specific peaks were observed that can be attributable to alumina (Al_2O_3) and zirconia (ZrO_2) implying that both might exist in amorphous forms at the temperature of synthesis.

3.1.3. FT-IR Spectra

The FTIR spectra of $\text{Al}_2\text{O}_3/\text{Fe}_3\text{O}_4/\text{ZrO}_2$ ternary oxide before and after adsorption of dyes and metals were measured to identify the nature and symmetry of interlayer anions and the presence of impurity phases by running the sample in KBr medium in the range of $4000\text{--}400\text{ cm}^{-1}$ [20] and the results are presented in figure 2.

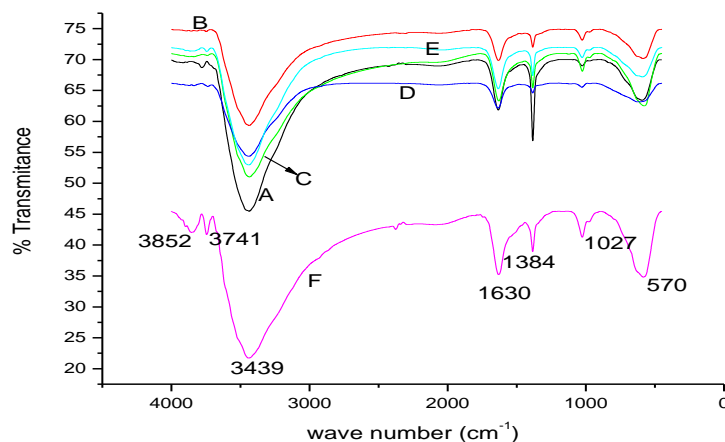


Figure 2. FT-IR spectrum of the As-synthesized nanosorbent (a = before adsorption, b = after Cu adsorption, C = after Ni adsorption, D = after Zn adsorption, e = after MB adsorption and f = after MO adsorption).

The strong and broad band at $3600\text{--}3100\text{ cm}^{-1}$ region (O-H stretching vibration) may be assigned for the presence of hydroxyl of coordinated water molecules [21]. The band at 1630 cm^{-1} primarily attributed

to the bending vibration of H-O-H [22]. When comparing the spectrum of $\text{Al}_2\text{O}_3/\text{Fe}_3\text{O}_4/\text{ZrO}_2$ ternary oxide before adsorption with the spectrum after adsorption, the long and sharp peak formed at 1384 cm^{-1} (surface hydroxyl group, M-OH) before adsorption was weakened and formation of short peaks were observed after adsorption. These results approved that the dyes and heavy metals were successfully adsorbed on the surface of $\text{Al}_2\text{O}_3/\text{Fe}_3\text{O}_4/\text{ZrO}_2$ ternary oxide [21]. The bands at 570 cm^{-1} may be assigned to M-O symmetrical stretching vibrations of the mixed metal [23].

3.1.4. SEM-EDX Analysis

Scanning electron microscopy coupled with energy dispersive X-ray detector (SEM-EDX) was used to observe the morphology, particle size and composition of Al-Fe-Zr ternary oxide nanosorbent. SEM micrographs (Figure 3a) revealed that the particles are generally characterized as of flake morphology, irregular shape, or uneven and rough with abundant protuberances and lots of pores which favored the adsorption of methyl orange, methylene blue, copper, nickel and zink. X-ray energy dispersive analysis of the imaged area (Figure 3b) shows a relative concentration of aluminum, iron and zirconia are 4.8%, 89.9 and 2%, respectively.

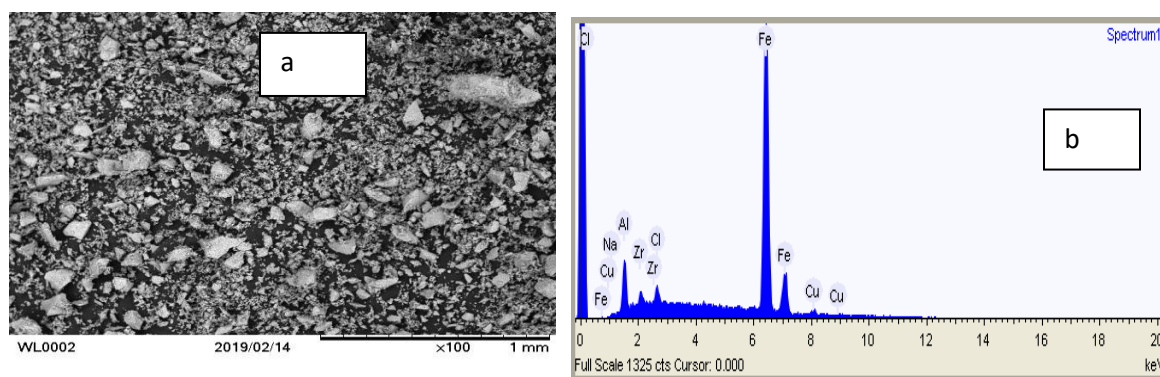


Figure 3. SEM (a) and EDX (b) images of $\text{Al}_2\text{O}_3/\text{Fe}_3\text{O}_4/\text{ZrO}_2$ calcined at 60°C for 24 h.

3.2. pH of Point Zero Charge (pHpzc) and Effect of pH Study

Point of zero charge for a given mineral surface is the pH at which that surface has a net neutral charge. The significance of this kind of plot is that a given mineral surface will have positive charge at solution pH values less than the pzc and thus be a surface on which anions may adsorb. On the other hand, that mineral surface will have negative charge at solution pH values greater than the pzc and thus be a surface on which cations may adsorb [14]. For this particular work, the pHpzc value is found to be 5.78 (figure 4). Amongst the various physical parameters, the most significant factor influencing the efficiency of an adsorbent in wastewater treatment is the pH of the solution. The effectiveness of adsorption is reliant on the pH of the medium, since diversity in pH prompts variations in the surface properties of the adsorbent and in the degree of ionization of the adsorbate molecule. Hence, it is necessary to determine pH values, where maximum adsorption will take place [24]. According to figure 1, the maximum adsorption for MO, Cu, Zn and Ni was achieved at pH 6 (94.03, 88.57, 87.73, and 85.41 % respectively) and that of MB was obtained at pH 4 (95.91%). The adsorption decreased back at higher pH. The adsorption behavior under different pH shown from our results as well other results from previous authors indicated, in general, that there are electrostatic interactions between the adsorbent and the adsorbates [25]. The

dye removal efficiency of $\text{Al}_2\text{O}_3/\text{Fe}_3\text{O}_4/\text{ZrO}_2$ obtained in this study is higher than the color removal efficiency of Fe_3O_4 studied by Hariani et al [26] at pH solution 5.

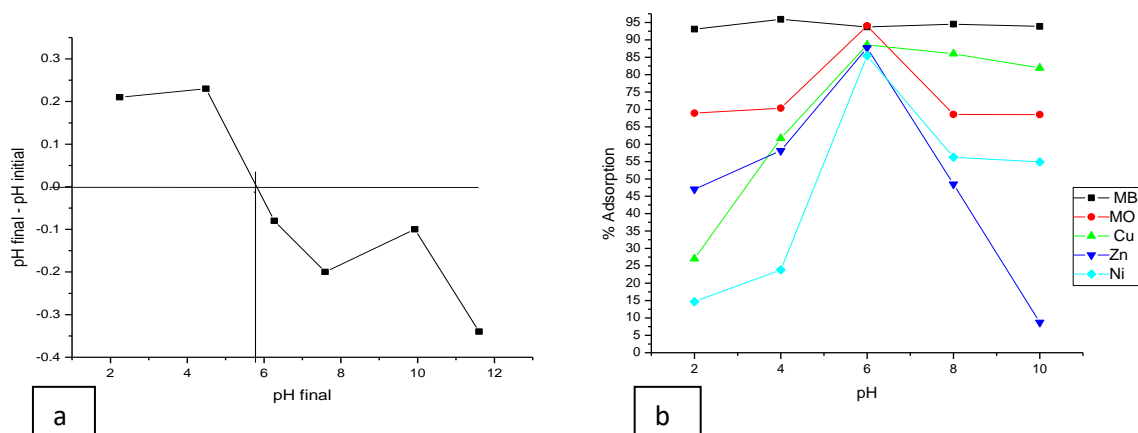


Figure 4. Plot for pH of point zero charge determination (a) and effect of pH (b) on MB, MO, Cu, Zn and Ni adsorption on to $\text{Al}_2\text{O}_3/\text{Fe}_3\text{O}_4/\text{ZrO}_2$ nanoparticle (dose = 0.1g, conc = 30 mg/L, speed = 120 rpm).

3.3. Effect of Adsorbent Dose

The result of adsorbent dose study is shown on figure 5. It was observed that the removal efficiency increased with an increase in adsorbent dose from 0.05 to 1 g for MB, MO and Zn and maximum adsorption of Cu was obtained at 0.5 g. This indicates that with increasing adsorbent dosage, more surface area was available for adsorption due to the increase in active site on the surface and thus making easier penetration of adsorbate to adsorption [26]. Maximum nickel adsorption was obtained at 0.05 g indicates that, small amount of $\text{Al}_2\text{O}_3/\text{Fe}_3\text{O}_4/\text{ZrO}_2$ nanoparticle is enough to remove it.

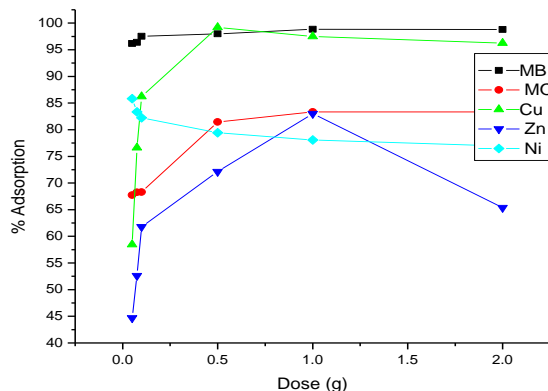


Figure 5. Plot for effect of dose on MB (pH = 4), MO, Cu, Zn and Ni sorption on to $\text{Al}_2\text{O}_3/\text{Fe}_3\text{O}_4/\text{ZrO}_2$ at initial concentration of 30 mg/L and contact time of 24 ((pH = 6, Speed = 120 rpm).

3.4. Effect of Contact Time

The result of effect of contact time was presented on figure 6. The removal efficiency for MB is maximum (97.81%) in the first four hour. The maximum adsorption of MO (99.1%) and Cu (99.74%) was obtained in the first 8 h and that of Zn (89.13%) and Ni (83.7%) was at 12 hour. The changes in the extent of adsorption might be due to the fact that initially all the adsorbent sites were free and the solute concentration was high. Later, the Ni, Zn and MB uptake by the adsorbent decreased significantly and that of Cu and MO slightly, due to decrease in the number of active sites [24].

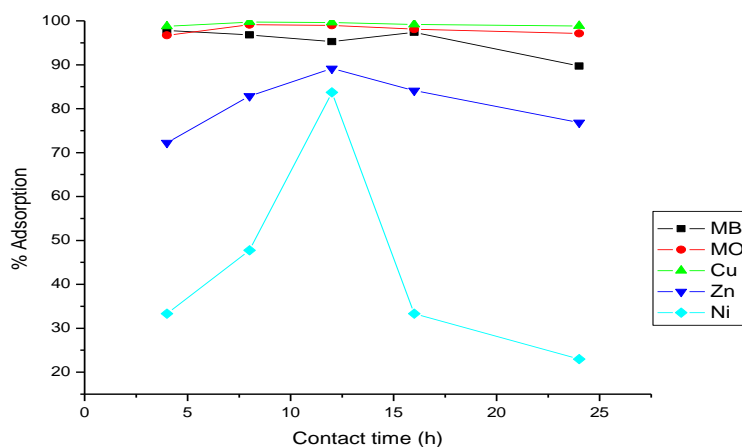


Figure 6. Plot for effect of contact time on MB (pH = 4, dose = 1g), MO (pH = 6, dose = 1g), Cu (pH = 6, dose 0.5 g), Zn (pH = 6, dose = 1g) and Ni (pH = 6, dose = 0.05g), adsorption at initial concentration of 30 mg/L and speed of 120 rpm.

3.5. Effect of Agitation Speed and Initial Concentration Study

The result of effect of agitation Speed and initial concentration study was presented on figure 7. Stirring is an important parameter in adsorption phenomena, influencing the distribution of the solute in the bulk solution and the formation of external boundary layer. MB, MO, Cu and Ni removal increased as the rate of stirring increases from 50 to 100 rpm, while the maximum adsorption of Zn was achieved at 120 rpm. The reason for the increase in the efficiency may be due to increase in the contact between adsorbate and adsorbent at higher speeds [27]. During further increase in agitation speed beyond optimum speed adsorption process decreased slightly for all analytes except that of MO which initially shows sharp decrease in adsorption.

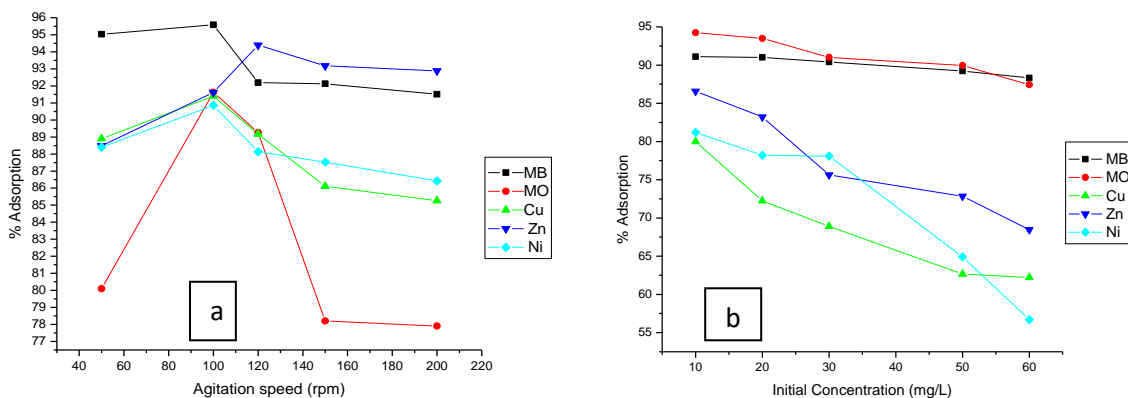


Figure 7. Plot for effect of Agitation Speed (a) and Initial Concentration (b) on MB, MO, Cu, Zn and Ni, adsorption on the as-synthesized nanosorbent at pre optimized conditions.

Concentration of adsorbate also affects the process of adsorption [28]. The maximum adsorption was obtained at 10 mg/L for both dyes and heavy metals. Further increase in the concentration of adsorbate indicated the decrease in % adsorption. At high-level concentrations, the available sites of adsorption become fewer. This behavior is connected with the competitive diffusion process of the ions through the micro channel and pores in $Al_2O_3/Fe_3O_4/ZrO_2$. This competitive will lock the inlet of channel on the surface and prevents the ions to pass deeply inside the nanoparticle [29].

3.6. Adsorption Isotherm Study

Adsorption from aqueous solutions involves concentration of the solute on the solid surface. The representation of the amount of solute adsorbed per unit of adsorbent (q) as a function of the equilibrium concentration of the solute in the bulk solution (C_e) at a constant pH and temperature is called an isotherm [30]. Several models can be used for the description of adsorption data with the Freundlich and Langmuir isotherms being most commonly used. The Langmuir equation is useful for the estimation of maximum adsorption capacity corresponding to complete monolayer coverage and expressed by:

$$Q_e = \frac{Q_o b C_e}{1 + b C_e} \quad (4)$$

The Linearized form of equation:

$$\frac{C_e}{q_e} = \frac{1}{Q_o b} + \frac{C_e}{Q_o} \quad (5)$$

Q_o is the amount of adsorbate at complete monolayer coverage (mg/g) and gives the maximum sorption capacity of sorbent, C_e is the equilibrium concentration of adsorbate (mg/L) and b (L/mg) is Langmuir isotherm constant that relates to the energy of adsorption. The Langmuir constants Q_o and b can be calculated from the slope ($1/Q_o$) and intercept ($1/Q_o b$) of the plot C_e/q_e versus C_e respectively (figure 8).

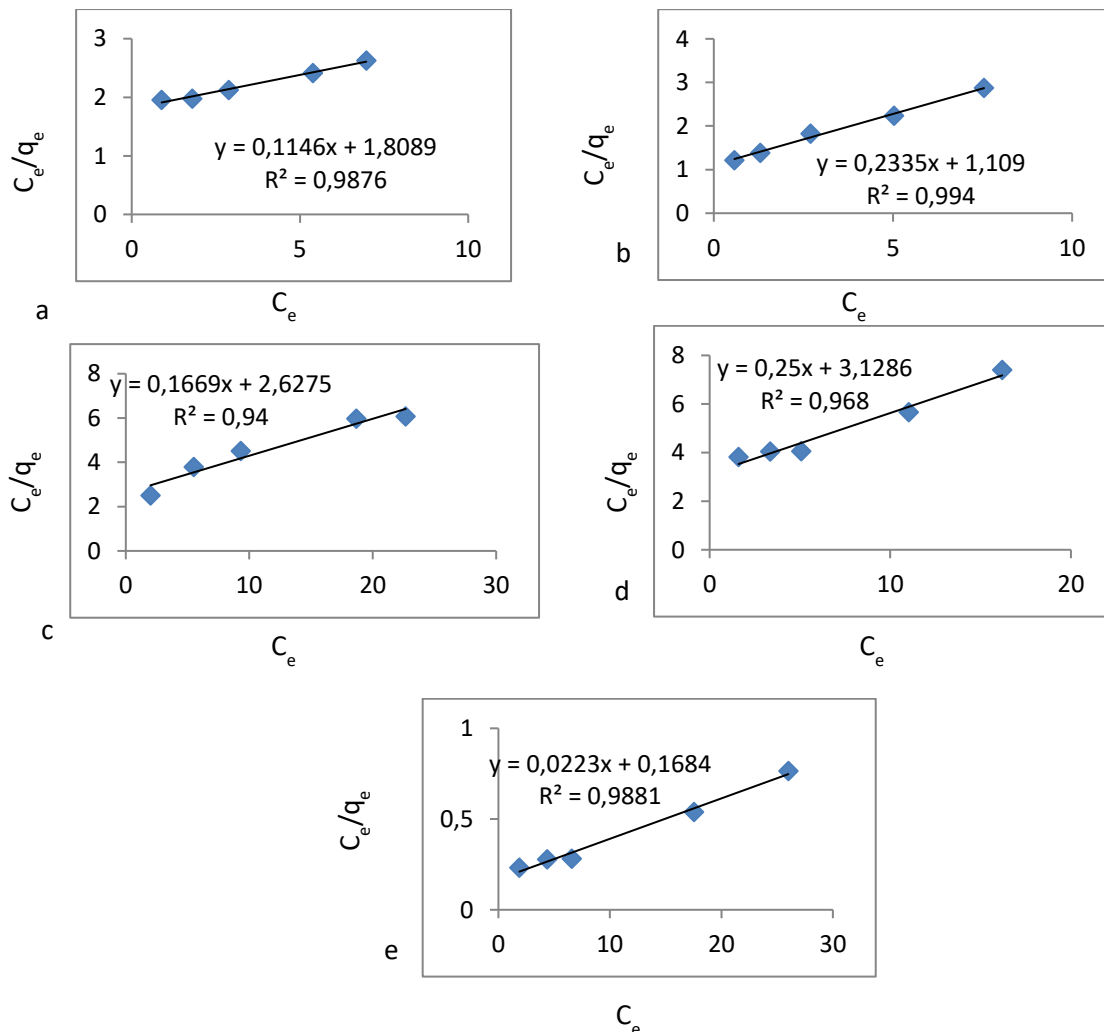


Figure 8. Plot for Langmuir adsorption isotherm study on MB (a), MO (b), Cu (c), Zn (d) and Ni (e) adsorption at initial concentration of 10 mg/L.

The Freundlich adsorption isotherm is the most widely used mathematical description of adsorption in aqueous systems. The Freundlich equation is expressed as:

$$q = KCe^{1/n} \tag{6}$$

where q = amount of solute adsorbed per unit weight of adsorbent (g/mg), C_e = equilibrium concentration of the solute (mg/L) K , $1/n$ = isotherm constants. K is the measure of adsorption capacity and $1/n$ is the measure of adsorption intensity. Upon linearization, the equation takes the form:

$$\log q = \log K + 1/n \log C_e \tag{7}$$

If $1/n$ is close to 1, this indicates a high adsorptive capacity at high equilibrium concentrations, which rapidly diminishes at lower equilibrium concentrations covered by the isotherm. Relatively flats slope, i.e. $1/n \ll 1$, indicates that adsorption capacity is only slightly reduced at the lower equilibrium concentrations. As the Freundlich equation indicates, the adsorptive capacity q is a function of the equilibrium concentration of the solute. Therefore, higher capacities are obtained at higher equilibrium concentrations [31]. The Freundlich isotherm constants $1/n$ and K_f can be calculated from the slope and intercept of the plot $\log q_e$ vs $\log C_e$. For this study, the Freundlich isotherm adsorption model for adsorption of MB, MO, Cu, Zn and Ni onto $Al_2O_3/Fe_3O_4/ZrO_2$ ternary nanocomposite was as indicated in figure 9.

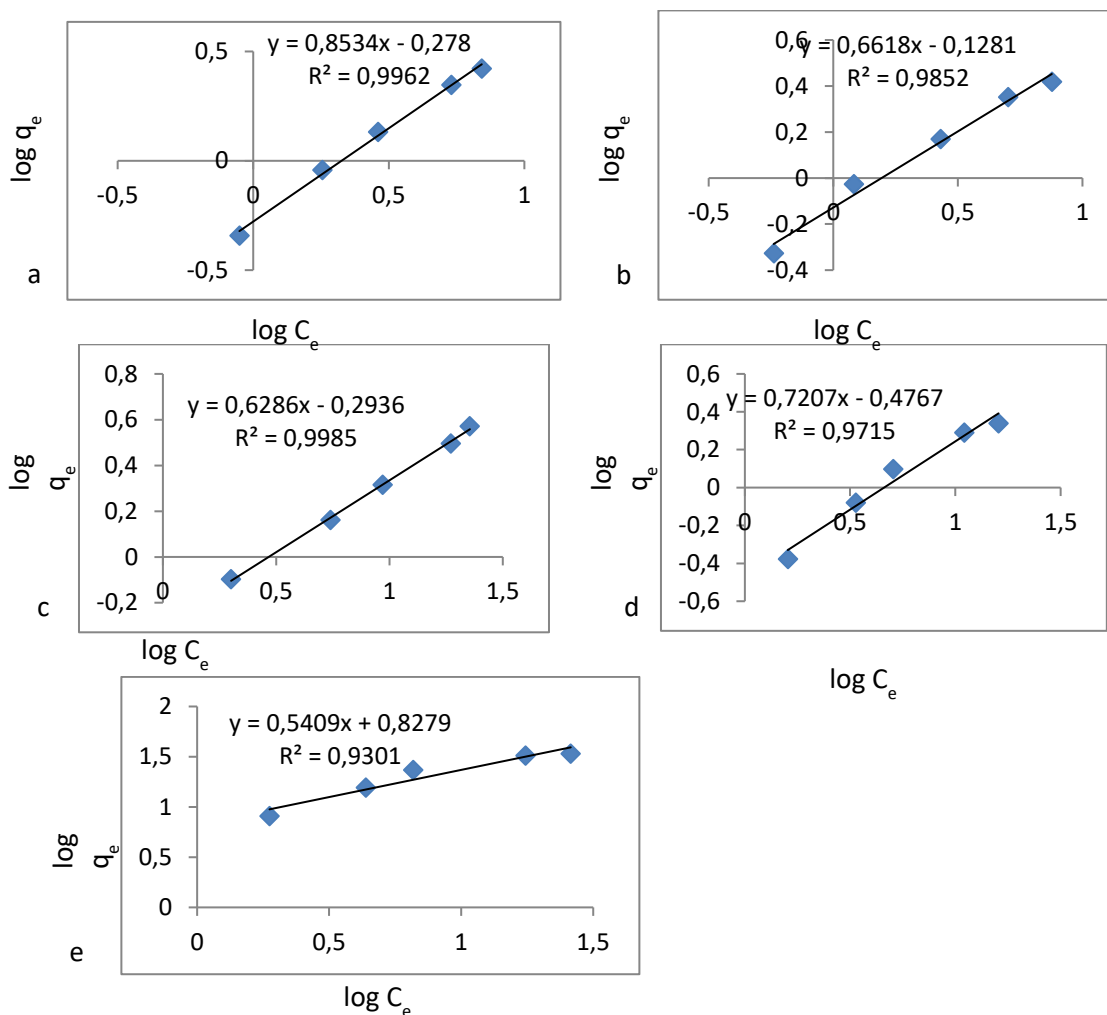


Figure 9. Plot for Freundlich adsorption isotherm study on MB (a), MO (b), Cu (c), Zn (d) and Ni (e) adsorption at initial concentration of 10 mg/L.

In general, K_f value increases the adsorption capacity for a given adsorbate increases. The adsorption coefficient, K_f of Nickel on $Al_2O_3/Fe_3O_4/ZrO_2$ is high compared to the other. This indicates that the rate of adsorption of Ni is rapid [9].

Table 1. Langmuir and Freundlich constants for MB, MO, Cu, Zn and Ni adsorption onto $Al_2O_3/Fe_3O_4/ZrO_2$ ternary nanocomposite.

Analyte	Langmuir				Freundlich		
	Qo (mg/g)	b	RL	R ²	Kf	1/n	R ²
MB	8.8	0.063	0.613	0.987	0.533	0.853	0.996
MO	4.3	0.21	0.323	0.994	0.745	0.661	0.985
Cu	6.024	0.063	0.613	0.94	0.509	0.628	0.998
Zn	4	0.08	0.56	0.968	0.334	0.72	0.971
Ni	45.45	0.131	0.433	0.988	6.71	0.54	0.93

The Langmuir's and Freundlich's curves were interpreted with respect to correlation coefficient R^2 . Both models were able to sufficiently describe the sorption data of the elements (Table 1). This was evidenced by the fact that the R^2 values derived from linearised equation of both models, were very high (>0.9), indicating a significant relationship between the elements adsorbed by the nanoparticle and their corresponding concentration in the equilibrium solution. However, the adsorption of MB, Cu and Zn, better fits Freundlich's equation as R^2 is greater than that of Langmuir, whereas MO and Ni adsorption better fits Langmuir equation.

The feasibility of the isotherm can be tested by calculating the dimensionless constant, R_L expressed as:

$$R_L = \frac{1}{1 + bC_0} \quad (8)$$

The value of R_L indicates the type of isotherm: to be irreversible if ($R_L = 0$), favorable if ($0 < R_L < 1$), linear if ($R_L = 1$), or unfavorable for ($R_L > 1$) [32]. Thus, the calculated values of R_L for MB, MO, Cu, Zn and Ni adsorption on to Al-Fe-Zr ternary oxide were found to be between 0 and 1 (Table 1) which attributes that all reactions were favorable at standard room temperature for all R_L values.

3.7. Adsorption Kinetics

The determination of kinetics is vital for the design of adsorption systems and the reaction rate controlling step as the chemical reaction occurs [33]. Adsorption kinetics describes the relations between the amount of adsorbates adsorbed on the adsorbents (q_t) and the contact time (t). The commonly used adsorption kinetics includes the pseudo-first-order and pseudo-second-order kinetic model [34]. The pseudo-first order adsorption kinetic model is given as [35].

$$\log (q_e - q_t) = \log q_e - \frac{k_1}{2.303} t \quad (9)$$

Where, q_e and q_t are the amount of dyes/ metals adsorbed (mg/g) at equilibrium and at any time t (min) respectively. The adsorption rate constant k_1 was determined from the slope of the linear plot of $\log (q_e - q_t)$ versus t (i.e., $k_1 = -2.303 \times \text{slope}$) and q_e is obtained from intercept ($\log q_e = \text{intercept}$). The integrated form of pseudo second order adsorption kinetic model is expressed as [33]:

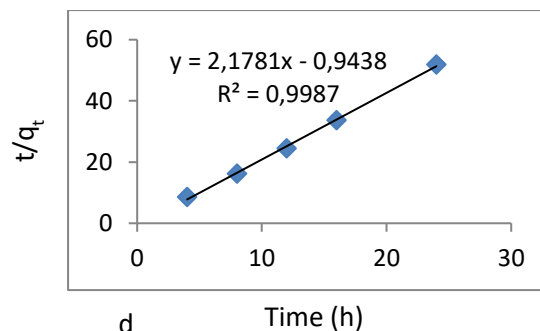
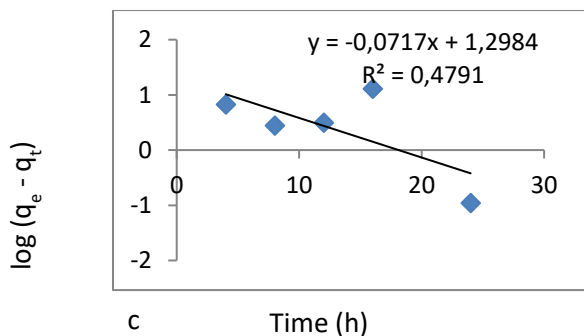
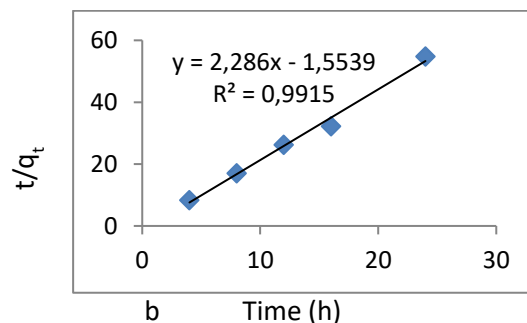
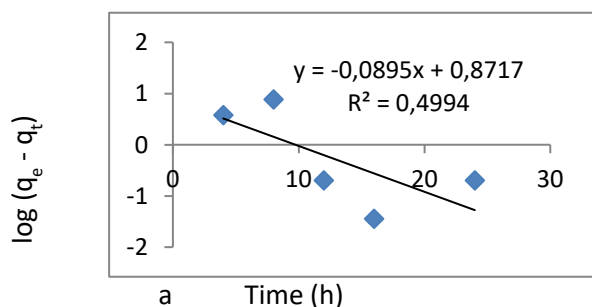
$$\frac{t}{q_t} = \frac{1}{k_2 q_e^2} + \frac{1}{q_e} t \quad (10)$$

k_2 which is (slope²/intercept) can be determined from plotting t/q_t against t based on above equation and the value of q_e is 1/slope.

Table 2. The values of parameters and coefficient of determination of kinetic models for MB, MO, Cu, Zn and Ni adsorption on to Al₂O₃/Fe₃O₄/ZrO₂ nanocomposite.

Analyte	q_e (mg/g) exp'tal	Pseudo-First Order			Pseudo-Second Order		
		q_e (mg/g)			q_e (mg/g)		
		calc.	K_1	R^2	calc.	K_2	R^2
MB	0.483	7.44	0.206	0.4994	0.437	-5.226	0.9915
MO	0.493	19.88	0.165	0.4791	0.459	-4.744	0.9987
Cu	0.99	1.613	0.047	0.4121	0.512	-3.821	0.9844
Zn	0.468	64.36	0.284	0.8286	0.387	-6.671	0.9935
Ni	13.66	28.774	0.06	0.903	21.74	-0.025	0.991

The pseudo second order kinetic model gave the best fit for experimental data as $R^2 > 0.98$ for adsorbates. Furthermore the calculated q_e values in case of pseudo second order kinetic model were close to experimental values. Thus, the adsorptions of these dyes and heavy metals on to Al₂O₃/Fe₃O₄/ZrO₂ can be best described by second order reaction.



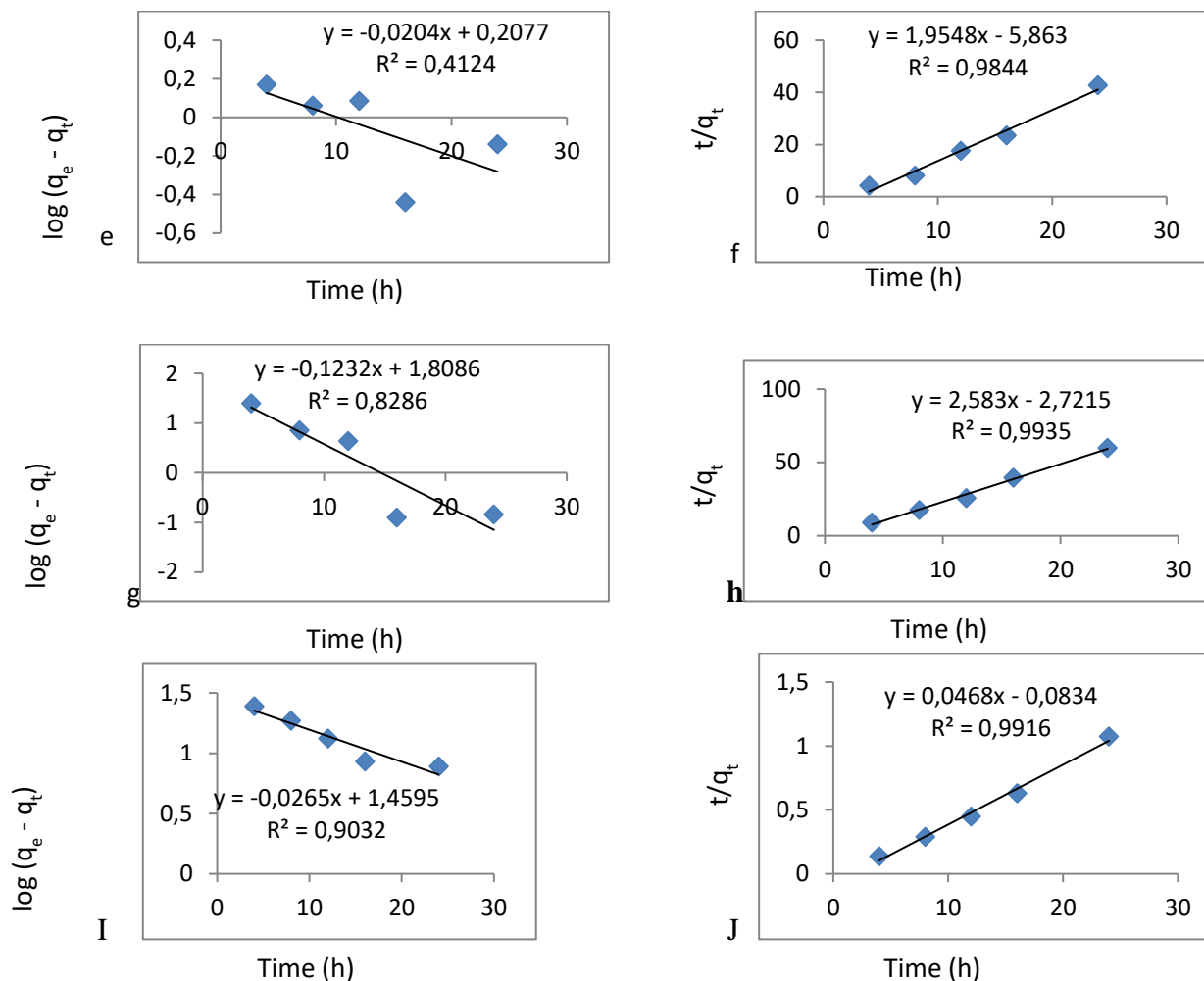


Figure 10. Plot for kinetic study for MB (a = first order, b= second order), MO (c = first order, d = second order), Cu (e = first order, f = second order), Zn (g = first order, h = second order) and Ni (I = first order, j = second order) adsorption on to the as-synthesized adsorbent.

3.8. Adsorption Thermodynamics Study

The standard free energy change (ΔG), enthalpy changes (ΔH) and entropy change (ΔS) are the main thermodynamic characteristics of any adsorption system in equilibrium. Thermodynamic considerations of an adsorption process are necessary to conclude whether the process is spontaneous or not. The Gibbs free energy change, ΔG , is an indication of spontaneity of a chemical reaction and therefore is an important criterion for spontaneity. Both enthalpy and entropy factors must be considered in order to determine the Gibbs free energy of the process. The fundamental thermodynamic equation that relates all the three above parameters is the follows [36]:

$$\Delta G = \Delta H - T \Delta S \quad (11)$$

The free energy of adsorption, considering the adsorption equilibrium constant K is given by the following equation:

$$\Delta G = -RT \ln K_c \quad (12)$$

where, R is universal gas constant ($8.314 \text{ Jmol}^{-1}\text{K}^{-1}$), T is temperature in Kelvin and K_c is the equilibrium constant obtained from q_e/C_e , ΔH and ΔS can be determined from the plot of $\ln K_c$ versus T^{-1} by

computing their slope and intercept (i.e. $\Delta H = -\text{slope} \times R$ and $\Delta S = \text{intercept} \times R$). From equations (11) and (12) a relationship follows between $\ln K_c$ and T :

$$\ln K_c = \Delta S/R - \Delta H/TR \quad (13)$$

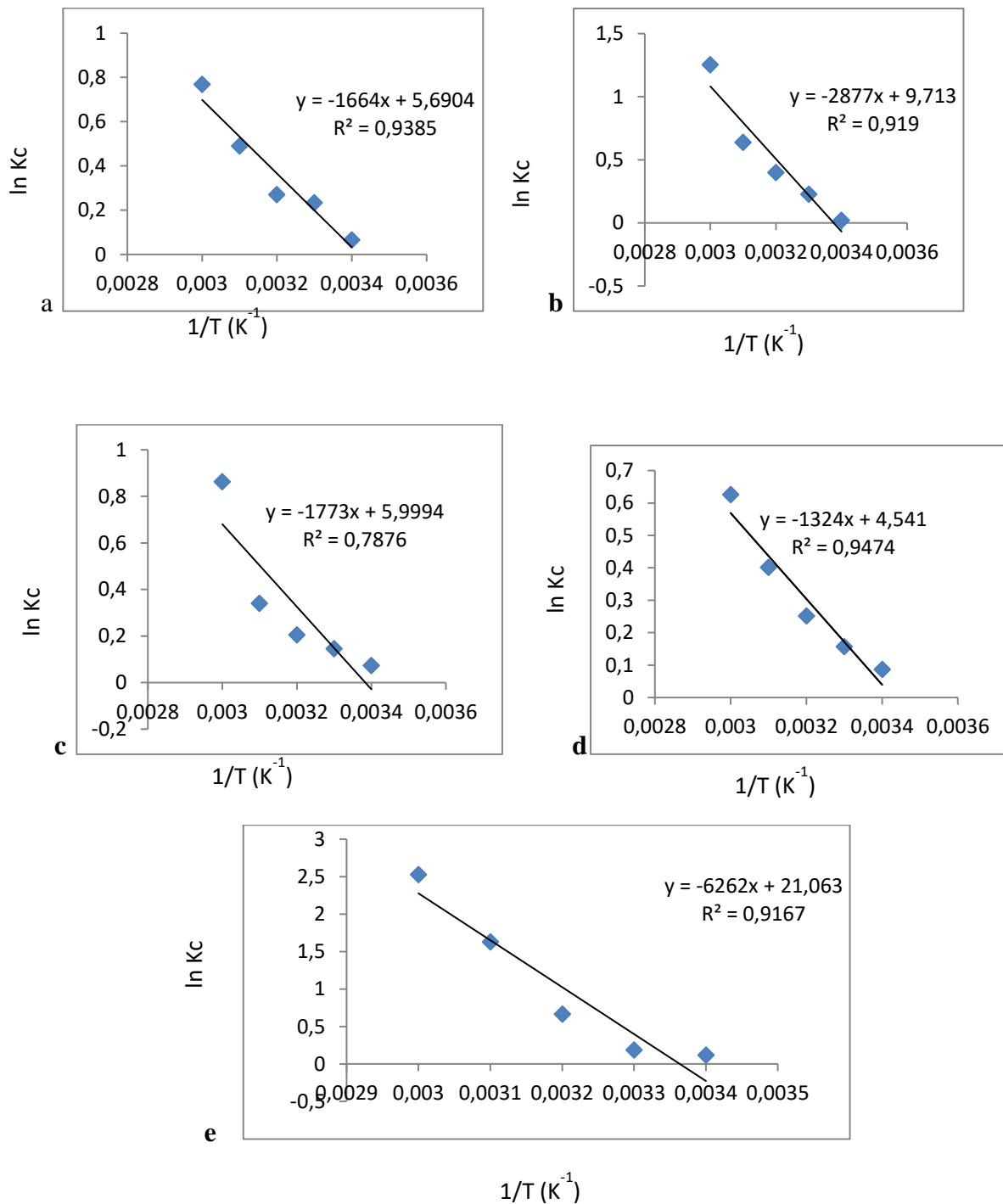


Figure 11. Plot for thermodynamic study for MB (a), MO (b), Cu (c), Zn (d) and Ni (e) adsorption on the nanosized adsorbent.

Table 3. Calculated thermodynamic constants of the MB, MO, Cu, Zn and Ni adsorption on to Al₂O₃/Fe₃O₄/ZrO₂ mixed oxide.

Analyte	T (K)	ln Kc	ΔG (J/mol)	ΔH (KJ/Mol)	ΔS (J/molK)
MB	293	0.019	-46.28	23919.4	80.73
	303	0.226	-569.33		
	313	0.399	-1038.3		
	323	0.637	-1710.6		
	333	1.252	-3466.2		
MO	293	0.074	-180.26	14740.7	49.87
	303	0.146	-367.79		
	313	0.205	-533.66		
	323	0.341	-913.73		
	333	0.863	-2389.3		
Cu	293	0.065	-158.34	13834.5	47.31
	303	0.234	-589.5		
	313	0.27	-702.6		
	323	0.49	-1315.9		
	333	0.769	-2129		
Zn	293	0.086	-209.5	11007.7	37.754
	303	0.157	-395.5		
	313	0.251	-653.17		
	323	0.401	-1076.9		
	333	0.626	-1733.1		
Ni	293	0.117	-285.01	52062.3	175.1
	303	0.186	-468.56		
	313	0.665	-1730.5		
	323	1.628	-4371.9		
	333	2.527	-6996.2		

The adsorption of these dyes and heavy metals increased with increasing temperature indicates that a high temperature favors the adsorption process. The enhancement in adsorption with temperature may

be attributed to increase in number of active surface sites available for adsorption on each adsorbent, increase in the porosity and in the total pore volume of the adsorbent. An increasing number of molecules may also acquire sufficient energy to undergo interaction with active sites at the surface. It is clear that the sorption of dyes/heavy metals on this sorbents is an endothermic process and spontaneous as indicated by positive ΔH and negative ΔG values respectively. The positive value of ΔS shows increased randomness at the solid-solution interface during the adsorption of dyes/metal ion on the adsorbent [9; 37].

3.9. Desorption Studies

Desorption studies help to elucidate the nature of adsorption and recycling of the spent adsorbent. The effect of various reagents (HCL, NaOH and DW) was checked for desorption studies and given on [table 4](#).

Table 4. Percentage desorption of different eluents

Analyte	Eluent	% desorption
MB	HCl	95.08
	NaOH	93.5
	DW	88.96
MO	HCl	86.5
	NaOH	79
	DW	72.5
Cu	HCl	64.9
	NaOH	94.07
	DW	87.05
Ni	HCl	71.68
	NaOH	91.46
	DW	80.01
Zn	HCl	80.05
	NaOH	85.77
	DW	83.26

The results indicate that hydrochloric acid is a better reagent for desorption of the two dyes, because we could get more than 85% removal of adsorbed dyes. On the other hand, the desorption of the metal ions is better in case of NaOH since the percent of desorption is greater than 85% ([table 4](#)). The results also indicate that all of the eluents used can desorb these dyes and heavy metals. The desorption of metal ion by mineral acids and alkaline medium indicates that the metal ion was adsorbed onto $Al_2O_3/F_3O_4/ZrO_2$ through physisorption as well as by chemisorptions mechanisms [9].

3.10. Application to Real Water Sample

The concentration of the metals in the waste water samples before and after using the adsorbent was determined as indicated on table 5. For Organic dyes contaminated aqueous solutions were artificially prepared by adding 5 ppm into the water. The application of nanosorbent was done at pre optimized condition.

Table 5. Data for applicability on water samples for triplicate experiment.

Analyte	Initial concentration in Water sample	Conc. after using Adsorbent	Initial Conc. added	Concentration after using adsorbent
Zn	0.61±0.041	0.021±0.015	5	0.114±0.03
Cu	0.264±0.014	0.014±0.032	5	0.105±0.086
Ni	0.621±0.056	0.025±0.032	5	0.027±0.032
MO	-	-	5	0.0105±0.002
MB	-	-	5	0.0113±0.010

The result indicates that the amount of the contaminants after using the adsorbent is very low comparing with the initial values indicates that the ability of $\text{Al}_2\text{O}_3/\text{Fe}_3\text{O}_4/\text{ZrO}_2$ to remove contaminants from wastewater is high.

Conclusion and Recommendation

The results of the present study indicate that $\text{Al}_2\text{O}_3/\text{Fe}_3\text{O}_4/\text{ZrO}_2$ nanocomposite is good sorbent for removal of MB, MO, Cu, Zn and Ni from waste water. The highest MO, Cu, Zn and Ni removals were obtained at pH 6 and removal of MB was obtained at pH 4. This suggested that pH has predominant effect on the adsorptive removal of contaminants from aqueous solution. Both Langmuir and Freundlich models were able to sufficiently describe the sorption data of the elements as indicated by R^2 values of > 0.9 . However, the adsorption of MB, Cu and Zn, better fits Freundlich's equation as R^2 is greater than that of Langmuir, whereas MO and Ni adsorption better fits Langmuir equation. The adsorption kinetic result indicated that the adsorption of all elements on the synthesized $\text{Al}_2\text{O}_3/\text{Fe}_3\text{O}_4/\text{ZrO}_2$ nanocomposite follows pseudo second order reaction. Adsorptions of all elements are spontaneous and endothermic as it was confirmed by negative values of ΔG and positive value of ΔH respectively.

Since $\text{Al}_2\text{O}_3/\text{Fe}_3\text{O}_4/\text{ZrO}_2$ used as a viable technology for MB, MO, Cu, Zn and Ni removal from wastewater we recommend that Optimize the removal efficiency of the nano sized adsorbent through continuous column experiment and carry out the research on the removal capacity of this nanosorbent for other contaminants is important.

Acknowledgement-The financial support from Research and Extension Office and Central Laboratory of Haramaya University are gratefully acknowledged.

References

1. H. Sarkheil, F. Noormohammadi, R.A. Rezaei, K.M. Borujeni. Dye pollution removal from mining and industrial wastewaters using chitson nanoparticles, *Environment and Biological Sciences*. 2 (2014) 37-43.
2. N. Dalali, M. Khoramnezhad, M. Habibizadeh, M. Faraji. Magnetic Removal of Acidic Dyes from Waste Waters Using Surfactant-Coated Magnetite Nanoparticles: Optimization of Process by Taguchi Method, *Environmental and Agriculture Engineering*. 15 (2011) 89-93.
3. O.B. Akpor, O.G. Ohiobor, D.T. Olaolu. Heavy metal pollutants in wastewater effluents: Sources, effects and remediation, *Advances in Bioscience and Bioengineering*. 2(2014) 37-43.
4. M.E. Etoriki, M. El-Rais, T.H. Mahabbis, M.N. Moussa. Removal of Some Heavy Metals from Wastewater by Using of Fava Beans, *American Journal of Analytical Chemistry*. 5 (2014) 225-23.
5. G. Patel, S. Pal, Menon. Removal of fluoride from aqueous solutions by CaO nanoparticles, *Separation Science Technology*. 44(2008) 2806-2826.
6. J. Rinku, S. Shripa, P. Hemant. Removal of malachite green dye from aqueous solution using magnetic activated carbon, *Research Journal of Chemical Sciences*. 5 (2015) 38-4.
7. M.P. Watts, V.S. Coker, S.A. Parry, R.A.D. Pattrick, R.A.P. Thomas, R. Kalin, J.R. Lloyd. Biogenic nano-magnetite and nano-zero valent iron treatment of alkaline Cr(VI) leachate and chromite ore processing residue, *Applied Geochemistry*. 54 (2015)27–42.
8. C. Jiang, and A.D. Xiao, D.A. Nanosized Zirconium Dioxide Particles as an Efficient Sorbent for Lead Removal in Waters, *Adv. Mater. Res.* (2014) 926–930, 166–169.
9. K. Kavitha, M. M. Senthamilselvi, S. Arivoli. Studies on the isotherms, kinetics and thermodynamics of adsorption of nickel (II) on low cost material, *Der Chemica Sinica*. 5 (2014) 135-146.
10. D. Anamaria, P. Mariana, C. Bogdan. Tailored and Functionalized Magnetite Particles for Biomedical and Industrial Applications. Prof. Sabar Hutagalung, ISBN: 978-953-51-0193-2 (2012).
11. K. Fekadu. Synthesis and Characterization of Al₂O₃/Fe₃O₄/ZrO₂ Hetero junction Ternary Oxides Nanocomposite for Nitrate Sorption from Aqueous Solution. Thesis, Haramaya University, Ethiopia (2015).
12. G. Vijayakumar, R. Tamilarasan, M. Dharmendirakuma. Adsorption, Kinetic, Equilibrium and Thermodynamic studies on the removal of basic dye Rhodamine-B from aqueous solution by the use of natural adsorbent perlite, *Journal of Material Environmental Sciences*. 1 (2012) 2028-2508.
13. T. Yan, L. Wang. Dye uptake by Compost, *Journal of Bio Resources*. 8 (2013) 4722-4734.
14. S. Panumati, K. Chudecha, P. Vankhaew. Adsorption of phenol from diluted aqueous solutions by activated carbons obtained from bagasse, oil palm shell and pericarp of rubber fruit, *Journal of Science Technology*. 30(2008) 185-189.

15. A.S. Tofik, M.T. Abi, K.T. Tesfahun. Synthesis, characterization and analytical evaluation of nano-sized iron/aluminum mixed oxide sorbent system for removal of phosphate from aqueous system, *Journal of Environmental Chemical Engineering*. 1(2016) 2458-2468.
16. M. Raka, D. Sirshendu. Adsorptive removal of nitrate from aqueous solution by polyacrylonitrile–alumina nanoparticle mixed matrix hollow-fiber membrane. *Journal of Membrane Science*, 466 (2014) 281– 292.
17. G. Fahmida, K. Yoshikazu, N. Akira and O. Kiyoshi. Preparation of alumina–iron oxide compounds by gel evaporation method and its simultaneous uptake properties for $\text{Ni}_2^+\text{NH}_4^+$ and H_2PO_4^- . *Journal of Hazardous Materials*. 169(2009) 697–702.
18. Y. Wang, L.X. Zhao and L.J. Yan. An application of nano-technology in environmental protection. *Shanghai Environmental Science*, 23 (2004) 178-181.
19. Z. Khayat and S. Khayat. Synthesis and Magnetic Properties Investigations of Fe_3O_4 Nanoparticles. *Proceedings of the 4th International Conference on Nanostructures (ICNS4)* 12-14 March, 2012, Kish Island, I.R. Iran.
20. A. Buzuayehu. Synthesis and Characterization of Nanosized Fe/Al/Mn mixed Oxide sorbent System for removal of Phosphate from Aqueous Solution. MSc Thesis, Haramaya University, Haramaya, Ethiopia, 2012.
21. F. Long, L.J. Gong, M.G. Zeng and L. Chen. Removal of phosphate from aqueous solution by magnetic Fe-Zr binary oxide. *Journal of Chemical Engineering*. 171 (2011) 448-455.
22. L. Jianbo, L. Huijuan, X. Zaho, S. Liping and Q. Jihu. Adsorptive removal of phosphate by a nanostructured Fe-Al-Mn trimetal oxide sorbent. *Powder Technology*. 233 (2013) 146-154.
23. S.G. Zhang, J.H. Liu, P.R. Liu and H.J. Qu. Removal of phosphate from water by a Fe–Mn binary oxide adsorbent. *Journal of Colloid Interface Sciences*. 335 (2007) 168-174.
24. S. Waheed, S. J. Attar. Equilibrium analysis for Batch studies of Adsorption of fluoride in water using activated alumina rand 6S1-X, *International Journal of Chemical Science*. 6 (2008) 900-902
25. 18. K.A. Saad, M.A. Amr, D.T. Hadi, R.S.Arar, M.M.AL-Sulaiti, T.A. Abdulmalik, N.M. Alsahamary, J.C. Kwak. Iron oxide nanoparticles: applicability for heavy metal removal from contaminated water, *Arab Journal of Nuclear Sciences and Applications*. 45 (2012) 335-346.
26. L.P. Hariani, M.Faizal, R. Marsi, D. Setiabudidaya. Synthesis and Properties of Fe_3O_4 Nanoparticles by Co-precipitation Method to remove Procion Dye, *International Journal of Environmental Science and Development*. 4 (2013) 336-340.
27. A. Goswami, K.M. Purkait. The defluoridation of water by acidic alumina, *Journal of Chemical Engineering Research and Design*. 9(2012) 2316–2324.
28. C. Devanand, D. Abishek, S.B. Sudipta, P. Liny, Krishna. Adsorption of Fluoride from water using *Spirulina platensis* and its Measurement using Fluoride Ion Selective Electrode, *Research Journal of Chemical Sciences*. 4(2014) 41- 44.
29. Z. Al-Anber, M. Al-Anber. Thermodynamics and Kinetic Studies of Iron (III) Adsorption by Olive Cake in a Batch System, *Journal of Mexican Chemical Society*. 52 (2008) 108-115.
30. J.C. Schippers, B. Petrusevski, S. K. Sharma, G.L. Amy. Module ground water resources And Treatment, Unesco-IHE, Delft (2007).
31. S.D. Faust, O.M.Aly, O.M. Chemistry of Water Treatment. Second edition, Lewis publisher, Boca Raton (1988).

32. T.W. Weber, and R. K. Chakkravorti. Pore and solid diffusion models for fixed -bed adsorbers, *AIChE J.* 20(1974) 228.
33. M. Matouq, N. Jildeh, M. Qtaishat, M. Hindiyeh, M.Q.A. Syouf. The adsorption kinetics and modeling for heavy metals removal from wastewater by Moringa pods, *Journal of Environmental Chemical Engineering.* 3 (2015) 775–784.
34. A. Ç Avu, G.L. Gu Rdag. Noncompetitive Removal of Heavy Metal Ions from Aqueous Solutions by Poly [2-(acrylamido)-2-methyl-1-propanesulfonic acid-co-itaconic acid] Hydrogel, *Industrial and Engineering Chemistry Research.* 48 (2016) 2652–2658.
35. A.M. Farhan, N.M. Salem, A.H. Al-Dujaili, A.M. Awwad. Biosorption Studies of Cr (VI) Ions from Electroplating Wastewater by Walnut Shell Powder, *American Journal of Environmental Engineering.* 2 (2012) 188–195.
36. L.A. Rodrigues, M.C.P. Silva. An investigation of phosphate adsorption from aqueous solution onto hydrous niobium oxide prepared by co-precipitation method, *Colloids Surface A.* 334 (2008) 191–196.
37. A. Battacharya, C. Venkobachar. Removal of Cadmium by Low Cost Adsorbents, *Journal of American Civil Engineering.* 110 (1984) 110-116.

(2020) ; <http://www.jmaterenvirosci.com>